ACS APPLIED MATERIALS & INTERFACES

Research Article

www.acsami.org

Designed Short RGD Peptides for One-Pot Aqueous Synthesis of Integrin-Binding CdTe and CdZnTe Quantum Dots

Hua He,[†] Min Feng,[†] Jing Hu,[†] Cuixia Chen,[†] Jiqian Wang,[†] Xiaojuan Wang,[†] Hai Xu,*[,†] and Jian R. Lu*[,‡]

[†]State Key Laboratory of Heavy Oil Processing and the Centre for Bioengineering and Biotechnology, China University of Petroleum (East China), 66 Changjiang West Road, Qingdao 266580, China

[‡]Biological Physics Laboratory, School of Physics and Astronomy, University of Manchester, Schuster Building, Manchester M13 9PL, United Kingdom

Supporting Information

ABSTRACT: We have designed a series of short RGD peptide ligands and developed one-pot aqueous synthesis of integrin-binding CdTe and CdZnTe quantum dots (QDs). We first examined the effects of different RGD peptides, including RGDS, CRGDS, Ac-CRGDS, CRGDS-$CONH_2$, Ac-CRGDS-$CONH_2$, RGDSC, CCRGDS, and CCCRGDS, on the synthesis of CdTe QDs. CRGDS were found to be the optimal ligand, providing the CdTe QDs with well-defined wavelength ranges (500−650 nm) and relatively high photoluminescence quantum yields (up to 15%). The key synthesis parameters (the pH value of the Cd^{2+}-RGD precursors and the molar ratio of RGD/Cd^{2+}) were assessed. In order to further improve the optical properties of the RGD-capped QDs, zinc was then incorporated by the simultaneous reaction of Cd^{2+} and Zn^{2+} with NaHTe. By using a mixture of CRGDS and cysteine as the stabilizer, the quantum yields of CdZnTe alloy QDs reached as high as 60% without any post-treatment, and they also showed excellent stability against time, pH, and salinity. Note that these properties could not be obtained with CRGDS or cysteine alone as the stabilizer. Finally, we demonstrated that the RGD-capped QDs preferentially bind to cell surfaces because of the specific recognition of the RGD sequence to cell surface integrin receptors. Our synthesis strategy based on RGD peptides thus represents a convenient route for opening up QD technologies for cell-specific tagging and labeling applicable to a wide range of diagnostics and therapy.

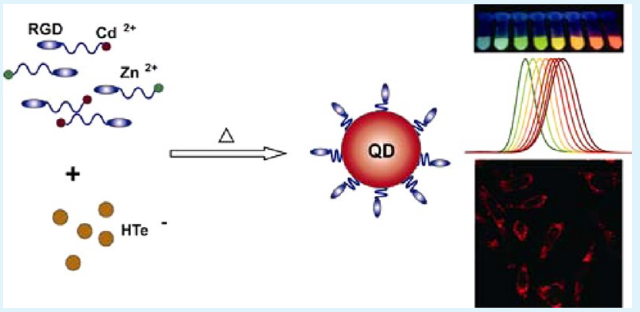

KEYWORDS: *quantum dots, RGD peptides, CdTe, CdZnTe, biorecognition*

1. INTRODUCTION

Colloidal quantum dots (QDs) have attracted enormous attention because of their unusual optical properties and great potential in diverse biological applications.[1−3] Most of the currently used QDs are prepared in an organic phase and are coated with hydrophobic organic ligands such as trioctylphosphine oxide.[4,5] To produce water-soluble QDs, which are compatible with biological systems, further surface modification is a prerequisite for the as-prepared QDs, typically through encapsulation with amphiphilic polymers[6−8] or exchange with hydrophilic thiol ligands.[9,10] However, these processes are often associated with adverse effects, such as a reduction in the quantum yield (QY) and stability[11,12] and a lack of control of the QD size.[13] Consequently, a simpler and more direct synthesis of QDs in aqueous solution has been extensively explored. Although short-chain thiol ligands such as thioglycolic acid (TGA) and 3-mercaptopropionic acid (MPA) have been used successfully in this regard,[14−17] the resulting particles often lack a biological interfacing capacity and further elaborate steps are thus needed to conjugate with biologically active molecules (e.g., streptavidin, antibodies, DNA oligonucleotides and aptamers, peptides) to achieve biological specificities.[18−21] These interfacial coupling chemistries are often complicated and time- and labor-intensive. Therefore, better and simpler QD surface functionalization approaches exploiting both optical advantages (high brightness, size tunability, and photostability) and biological specificity are essential to opening up QD-based technologies in diagnostics and therapy.

Kelley et al. have recently turned to nucleic acids as a versatile ligand set and found that these biological molecules, which can be engineered to bind DNA, protein, and cancer cell targets, are appropriate for the preparation of biocompatible semiconductor nanocrystals.[22] This approach can also be mimicked to develop a one-step synthesis of biofunctionalized CdS and CdTe nanocrystals in aqueous solution.[23−25] Although the optical properties of the as-prepared DNA- or RNA-capped

Received: September 16, 2012
Accepted: October 29, 2012
Published: October 29, 2012

 © 2012 American Chemical Society

QDs are not as good as those prepared in MPA or TGA solution, this approach suggests a new route to search for biomolecules for one-step syntheses of high-quality biofunctionalized QDs. There is, hence, a strong demand to develop new biomolecules and synthetic processes that can direct the synthesis of highly luminescent and stable QDs in aqueous solution and the surface grafting of biological functionalities to generate high biospecificity.

In this paper, we report the design and synthesis of a series of short heterobifunctional peptides for surface functionalization and stabilization of QDs. Peptides are small but carry the inherent advantage of easy customization for specific applications. By suitably combining diverse amino acid residues, simple peptide sequences with multiple functions can be designed.[26] Our designed peptides contain two different functional moieties, the side-chain thiol(s) of cysteine (Cys) residue(s) to bind to the QD surface and control the surface passivation and the RGD sequence (arginine-glycine-aspartic acid) pointing toward the surrounding aqueous solution and mediating the exemplary biorecognition.[27,28] Note that, although there have been some reports about RGD-functionalized QDs for targeted bioimaging, their conjugations to QDs were typically achieved through complex chemistries such as a biotin−streptavidin system,[29] maleimide-functionalized phospholipid encapsulation,[20] and heterobifunctional cross-linkers [e.g., 1-ethyl-3(3-dimethylaminopropyl)carbodiimide hydrochloride,[30] 4-maleimidobutyric acid *N*-succinimidyl ester,[31] and sulfosuccinimidyl 4-*N*-maleimidomethylcyclohexane-1-carboxylate[32]]. Here, with the designed RGD peptides as stabilizers, we have subsequently developed a simple one-pot aqueous synthesis route of biofunctionalized CdTe and CdZnTe QDs, and their preferential binding onto the cell surface via specific recognition between the RGD motif and integrin has also been demonstrated. The effects of different RGD peptides on the synthesis of CdTe QDs were examined. By optimization of RGD peptide primary structures and reaction conditions, the emission wavelengths of the RGD-capped CdTe QDs could be tuned from 500 to 650 nm, with QYs up to 15% and narrow full widths at half-maximum (fwhm) of 40−60 nm. In order to further improve the optical properties of QDs, the alloyed CdZnTe QDs was successfully prepared by the simultaneous reaction of Cd^{2+} and Zn^{2+} with NaHTe using a mixture of CRGDS and Cys as the stabilizer. The incorporation of Zn^{2+}, along with the combination of CRGDS and Cys as the stabilizer, greatly enhanced the QYs of QDs. Under optimized conditions, the QYs of CdZnTe alloy QDs were as high as 60% without any post-treatment. In addition, the alloy QDs were found to be biocompatible and stable under physiological conditions, making them suitable for cell-specific tagging and labeling. Finally, we demonstrated that the RGD-capped QDs preferentially bound to the cell surfaces because of the specific recognition of the RGD sequences to cell surface integrin receptors. The same synthetic route as that developed in this work enables similar surface attachment of more specific and more elaborate sequences or motifs to the QD surfaces, making it easy for the controlled targeting of specific cells or cellular organelles.

2. EXPERIMENTAL SECTION

2.1. Materials. Synthesis of the short RGD peptides was performed on a CEM Liberty microwave peptide synthesizer using the (fluorenylmethoxy)carbonyl solid-phase synthesis strategy from natural L-amino acids. The detailed synthetic procedures including peptide purification have been described in our previous work.[33−35] The purities were at least 95% for all peptides. The composition and purity of all peptides used were confirmed by matrix-assisted laser desorption ionization time-of-flight mass spectrometry and reversed-phase high-pressure liquid chromatography. Tellurium powder (99.997%), $CdCl_2$ (99.99+%), $ZnCl_2$ (99.995%), $NaBH_4$ (≥96%), and L-cysteine hydrochloride (≥98%) were purchased from Sigma-Aldrich and used as received. All solutions were prepared with ultrapure water (18.2 MΩ) purified on a Millipore System (Millipore, USA).

2.2. Synthesis of CdTe and CdZnTe QDs. A NaHTe solution was freshly prepared by dissolving 0.05 g of $NaBH_4$ in 2 mL of water, and then 0.04 g of tellurium powder was added to the $NaBH_4$ solution. This reaction was conducted at room temperature overnight in a syringe with a needle to help release the gas generated during the reaction, and the resulting NaHTe solution was diluted by injection into 23 mL of ultrapure water before use. For a typical CdTe QD synthesis, a Cd^{2+} peptide precursor solution was prepared by dissolving $CdCl_2$ and a given RGD peptide in ultrapure water and subsequently adjusting the pH to 8.5 with 1 M NaOH. The NaHTe solution was then injected into a N_2-saturated precursor solution under vigorous stirring. The typical molar ratio of Cd^{2+}, HTe^-, and peptide introduced was 4:1:10 in a total volume of 25 mL, with the final peptide concentration fixed at 1 mM. The resulting mixture was heated to 98 °C and refluxed at different times to control the size of the CdTe QDs. Aliquots of the reaction solution were taken out at regular intervals for further ultraviolet−visible (UV−vis) absorption and fluorescence characterization. For a typical ZnCdTe synthesis, Zn^{2+}-CRGDS and Cd^{2+}-CRGDS peptide precursor solutions were prepared by dissolving $ZnCl_2$, $CdCl_2$, and different stabilizers (CRGDS, Cys, or a mixture of the two) in ultrapure water and then adjusting the pH to 8.5 with 1 M NaOH. The typical molar ratio of zinc, cadmium, tellurium, and CRGDS peptide introduced was 2:2:1:10 in a total volume of 25 mL with a stabilizer concentration of 1 mM. All other manipulations were identical with those described in the synthesis of CdTe QDs.

2.3. Characterization. No postpreparative treatment was performed on any as-prepared samples for optical characterization. UV−vis absorption spectra were obtained using a Shimadzu UV-2450 spectrophotometer. Fluorescence spectra were recorded with a Hitachi F-2500 fluorescence spectrophotometer. All optical measurements were performed at room temperature under ambient conditions. The QY of CdTe QDs was measured using rhodamine 6G (QY = 95%) in an ethanol solution as a reference standard as described previously.[15,16] Transmission electron microscopy (TEM) samples were prepared by dropping the aqueous nanocrystals onto carbon-coated copper grids with excess solvent evaporated. TEM and high-resolution TEM (HRTEM) images were recorded on a JEM-2100 electron microscope (200 kV), which is equipped with an energy-dispersive spectrometry (EDS) system.

2.4. Cell Imaging. First, as-prepared RGD peptide-capped QDs were purified using Amicon Ultra-15 Centrifugal Filter Units (UFC900324, 3-kDa cutoff, Millipore Corp., USA) at 6000 rpm for 60 min. This procedure was repeated three times to remove all excess reagents and unbound peptides. Then, the purified QDs were resuspended in phosphate-buffered saline (PBS) and kept at 4 °C until use. Human cervical carcinoma HeLa cells, human promyelocytic leukemia HL60 cells, and human embryonic kidney 293 (HEK293) cells were purchased from the Cell Bank of the Shanghai Institute for Biological Science, Chinese Academy of Sciences (Shanghai, China). These cells were cultured with Iscove's modification of Dulbecco's medium supplemented with 10% fetal bovine serum in a humidified incubator at 37 °C in which the CO_2 level was kept constant at 5%. For HeLa cell imaging, a 1 mL solution with approximately 3000 cells was seeded onto a 10 mm sterile coverslip in a 24-well plate. After 24 h, the cells on the coverslip were rinsed three times with PBS (pH 7.4) and then incubated with approximately 200 nM (estimated according to ref 36) RGD peptide-capped QDs in PBS for about 30 min at room temperature. After that, the cells were washed three times with PBS to remove the unbound nanoparticles. Fluorescence images were

obtained with a Nikon A1 confocal laser scanning system (Nikon, Japan) with 488 nm argon laser excitation and 552−617 nm emission. For HL60 cell imaging, cells were washed twice with PBS, and cell suspensions were labeled with RGD-capped QDs for about 30 min at room temperature. After that, the cells were centrifuged at 2000 rpm for 5 min to remove unbound particles, and then the cells were washed twice and resuspended in PBS. A drop of the above solution was placed on top of a microscopic slide and sealed with a coverslip for observation under fluorescence microscopy (DMI3000B, Leica) equipped with a 100× oil immersion objective and a digital color camera (DFC490, Leica). HEK293 cells were used for MTT assays to assess the toxicity of QDs (see the Supporting Information).

3. RESULTS AND DISCUSSION

3.1. Design of RGD Peptides. Because the sequence of RGDS is more effective than RGD at binding integrin receptors,[27,37] the peptide tetramer was used in all of the peptides synthesized. To improve coordination between the RGD peptides and QD surface, Cys residue was incorporated into the sequence. The designed RGD peptides include CRGDS, RGDSC, Ac-CRGDS, CRGDS-$CONH_2$, Ac-CRGDS-$CONH_2$, CCRGDS, and CCCRGDS. Among them, multiple repeats of the Cys residue in tandem (CC or CCC sequences) were expected to enhance the peptide coverage on the QD surface, thereby improving the colloidal system stability.

3.2. Synthesis and Characterization of CdTe QDs. The synthesis of CdTe QDs was based on the reaction of cadmium chloride ($CdCl_2$) and sodium hydrotelluride (NaHTe). As a baseline control, when Cd^{2+} and HTe^- were mixed in the absence of additives, a dark precipitate formed immediately, indicating rapid condensation and crystallization into the bulk form. By contrast, upon the addition of HTe^- to Cd^{2+} solutions in the presence of the designed RGD peptides, colorless or slightly yellowish solutions formed immediately, depending on the peptides used, suggesting the crucial role of these peptides for stabilizing CdTe nanocrystals. When the resulting mixture solution was heated to 98 °C, CdTe QDs began to grow immediately. These different peptides exerted a distinct influence on the optical and chemical properties of the synthesized nanocrystals. A brief overview of the emission wavelength ranges, QYs, and stabilities of the CdTe QDs prepared is given in Table 1.

As indicated in Table 1 and Figure 1, CRGDS was the optimal ligand, providing the CdTe QDs with well-defined wavelength ranges, relatively high QYs, and good stability in aqueous solution. In contrast, other RGD peptides produced particles with weak luminescence and poor stability (Figures S1−S4 in the Supporting Information). Parts A and B of Figure 1 present the temporal evolution of the absorption spectra and corresponding photoluminescence (PL) spectra of the CdTe QDs prepared with CRGDS peptides, respectively. The inset shows a photograph of the corresponding CdTe QD solutions irradiated under a UV lamp. With prolonged growth time, the absorption and PL peak positions shifted to longer wavelengths. The emission peaks could be tuned from 500 to 650 nm, with fwhm increasing from 40 to 60 nm. The best QY of CdTe QDs produced by CRGDS was 15%. Note that the optical spectra and QYs shown in Figure 1 were measured from the crude solution of QD samples without purification. Under the same experimental conditions, the CdTe QDs as prepared from MPA, one of the most typical aqueous ligands, had the best QY of 36% (Figure S5 in the Supporting Information). In spite of higher QYs, the MPA-capped QDs must need further treatment

Table 1. Overview of the Optical Properties and Solution Stability of CdTe QDs Synthesized Using Different RGD Peptides as Stabilizers

RGD sequence[a]	wavelength range (nm)	typical QY[b] (%)	stability of CdTe QDs[c]
RGDS			
CRGDS	500−650	15	stable
RGDSC			
Ac-CRGDS	500−600	6	moderate
CRGDS-$CONH_2$	500−570	<1	unstable
Ac-CRGDS-$CONH_2$	500−550	<1	unstable
CCRGDS			
CCCRGDS			

[a]Each peptide is identified by its amino acid sequence, using one-letter amino acid abbreviations. All sequences are written from the N to C terminus. Ac- = N-terminal acetylation; -$CONH_2$ = C-terminal amidation. [b]The data were collected at 2 h of growth time. Note that the best QYs of CdTe QDs were typically achieved in the wavelength range of 540−570 nm, corresponding to a growth time of about 2−3 h. [c]"Stable" means that the colloidal dispersions of CdTe QDs were stable for months when stored in aqueous solution at 4 °C. "Moderate" means that the colloidal dispersions were stable for about 2 weeks. "Unstable" means that the QD samples produced precipitates during the growth process or after storage in aqueous solution for a few days.

for specific biological applications as indicated above, and such a process often greatly deteriorates their quality. TEM revealed that the CRGDS-capped CdTe QDs were spherical or slightly ellipsoidal with good monodispersity (Figure 1C). The existence of lattice planes on the HRTEM image (the inset in Figure 1C) is consistent with the crystallinity of these QDs. The size-distribution histogram (Figure 1D) indicates that the size of the particles emitted at 595 nm is 3.56 ± 0.65 nm. The representative TEM images of CdTe QDs emitted at 532 and 567 nm are also given, revealing their sizes as 2.73 ± 0.60 and 3.22 ± 0.43 nm, respectively (Figure S6 in the Supporting Information).

3.3. Influence of the RGD Sequence on CdTe QDs. The above results demonstrate that CdTe QDs could be successfully synthesized in aqueous solution through a very simple synthetic route. The key factor to this outcome arose from the surface passivation of QDs by the peptides. As indicated in Table 1, RGDS could not produce luminescent QDs because of the absence of the Cys residue. The failure of RGDSC indicates that the position of the Cys residue as the point of surface anchoring is important, with Cys on the N-terminal end offering far better QD stabilization. For CCRGDS and CCCRGDS, the original expectation of improving the QD quality by enhancing the surface coverage of peptides with more Cys residues was not achieved. Because of an increasing binding affinity for Cd atoms, the simultaneous presentation of two or more Cys residues on a peptide molecule might interfere with CdTe nanocrystal growth by competing with HTe^- and thus inhibiting the formation of luminescent CdTe QDs. In the synthesis of CdS nanocrystals also using Cys-containing peptides, Spoerke and Voigt reported the formation of rather small particles. These authors attributed the effect of the size reduction to the excessive capping of thiol groups.[38] In fact, the QD solution in the presence of CCCRGDS produced an extremely weak luminescence with an emission wavelength of about 450 nm in our experiments, irrespective of the

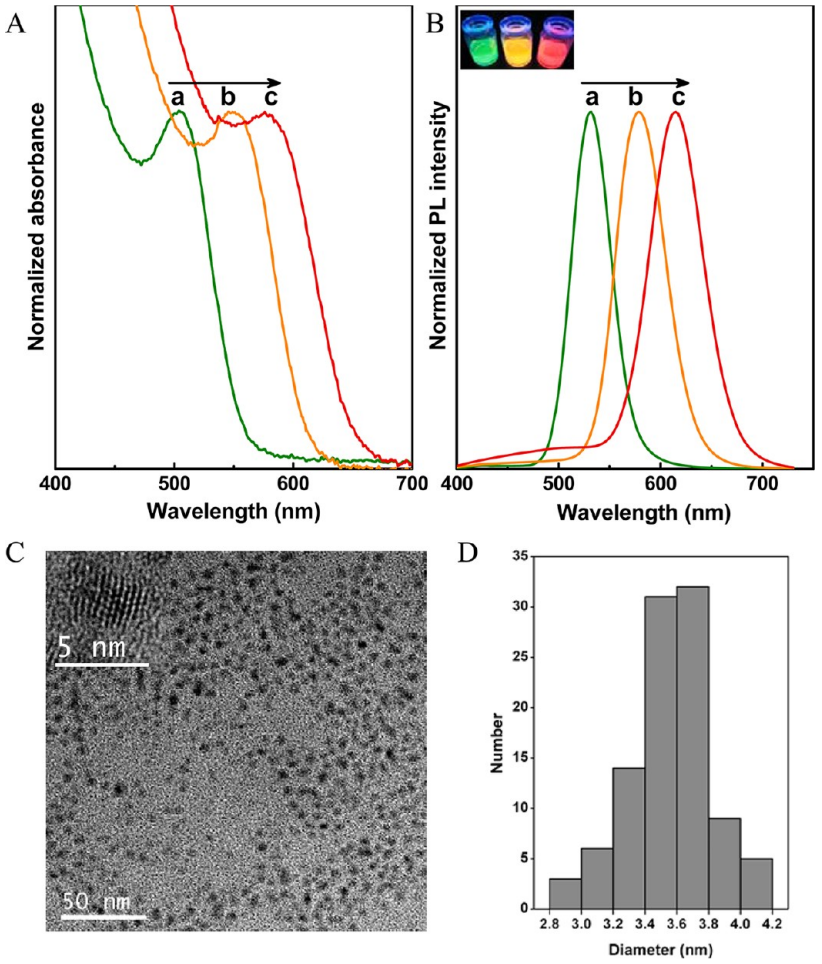

Figure 1. Temporal evolution of the absorption (A) and PL spectra (B) of CRGDS-capped CdTe QDs prepared at different growth times, respectively. The excitation wavelength for all PL spectra was 370 nm. In panels A and B, parts a–c correspond to the growth times of 1, 3, and 6 h, respectively. The emission wavelengths are 532, 578, and 615 nm, with QYs of 15%, 14%, and 9%, respectively. The inset gives a photograph of the corresponding solutions under irradiation with 365 nm of light from a UV lamp. (C) TEM and HRTEM (inset) images of CRGDS-capped CdTe QDs emitted at 595 nm. (D) Size-distribution histogram of the corresponding QDs, which was determined by measuring more than 100 particles from HRTEM images.

peptide/Cd^{2+} ratios (Figure S4 in the Supporting Information). This blue-shifted wavelength suggests the formation of very small particles, consistent with the observation by Spoerke and Voigt.

The C-terminal carboxyl and N-terminal amino groups of the peptides also exerted a marked influence on CdTe QDs. These can be seen from the optical properties of CdTe QDs produced by terminal capping peptides such as Ac-CRGDS, CRGDS-$CONH_2$, and Ac-CRGDS-$CONH_2$ (Table 1 and Figures S1–S3 in the Supporting Information). The absence of a terminal carboxyl or amino group or both significantly reduced the optical performances of CdTe QDs. Among the three peptides, Ac-CRGDS produced CdTe QDs with relatively strong luminescence with narrow and symmetric PL spectra, while CdTe QDs derived from Ac-CRGDS-$CONH_2$ were more prone to aggregation with the weakest luminescence. This observation implies that the terminal carboxyl and amino groups might form additional coordination with surface Cd atoms and thus enhance the emission intensity and colloidal stability of QDs, consistent with the previous observations reported.[39,40]

3.4. Influence of the pH and Molar Ratio of RGD/Cd^{2+}. The influence of key synthesis parameters such as the pH value of the Cd^{2+}-RGD precursors and the molar ratio of RGD/Cd^{2+} on the optical properties of QDs was assessed. In our experiments, the optimal pH was found to be around 8.5. At a low pH of 6.5, a slightly turbid suspension of particles was produced during the heating process because of the formation of QD aggregates at the pH close to the peptide's isoelectric points of ~6.1. This led to obvious nonzero baseline absorption, along with a dramatic decrease in the luminescence (Figure S7A in the Supporting Information). In contrast, at a high pH of 11.5, the growth rate increased dramatically, resulting in less clearly resolved excitonic absorption peak and wider PL fwhm values, indicating broader size distribution. For example, the CdTe QDs prepared at pH 8.5 by 40 min and 3 h of heating showed PL emission peaks at 505 and 552 nm, with fwhm values of 34 and 43 nm, respectively, while the CdTe QDs prepared at pH 11.5 by 40 min and 3 h of heating showed PL emission peaks at 527 and 632 nm with fwhm values of 50 and 74 nm, respectively. In addition, the optimal ratio of RGD/Cd^{2+} was found to be 2.5 with 1 mM RGD peptide, in broad agreement with the synthesis conditions of CdTe QDs using MPA or glutathione as the stabilizer.[15,41] At the low RGD/Cd^{2+} ratio of 1.25, a white precipitate appeared. When the molar ratio was increased to 5, the excitonic absorption peak of the

dx.doi.org/10.1021/am3020108 | ACS Appl. Mater. Interfaces 2012, 4, 6362–6370

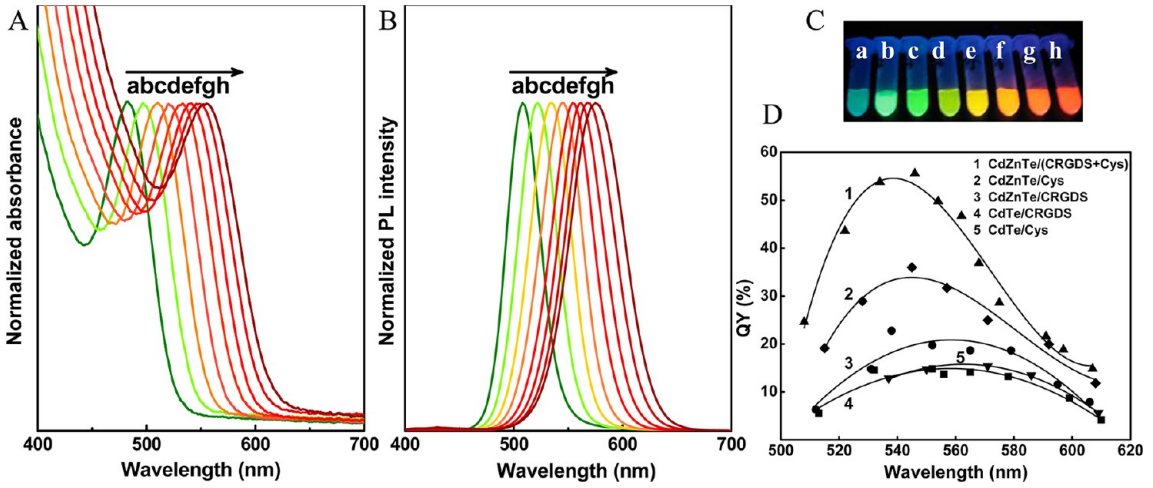

Figure 2. Temporal evolution of the absorption (A) and PL spectra (B) of (CRGDS + Cys)-capped CdZnTe QDs, respectively. Note that the ratio of CRGDS and Cys was 1:1. (C) Photograph of the corresponding QD aqueous solutions under irradiation with a UV lamp. (D) QY versus emission peak position of CdTe or CdZnTe QDs synthesized using different stabilizers.

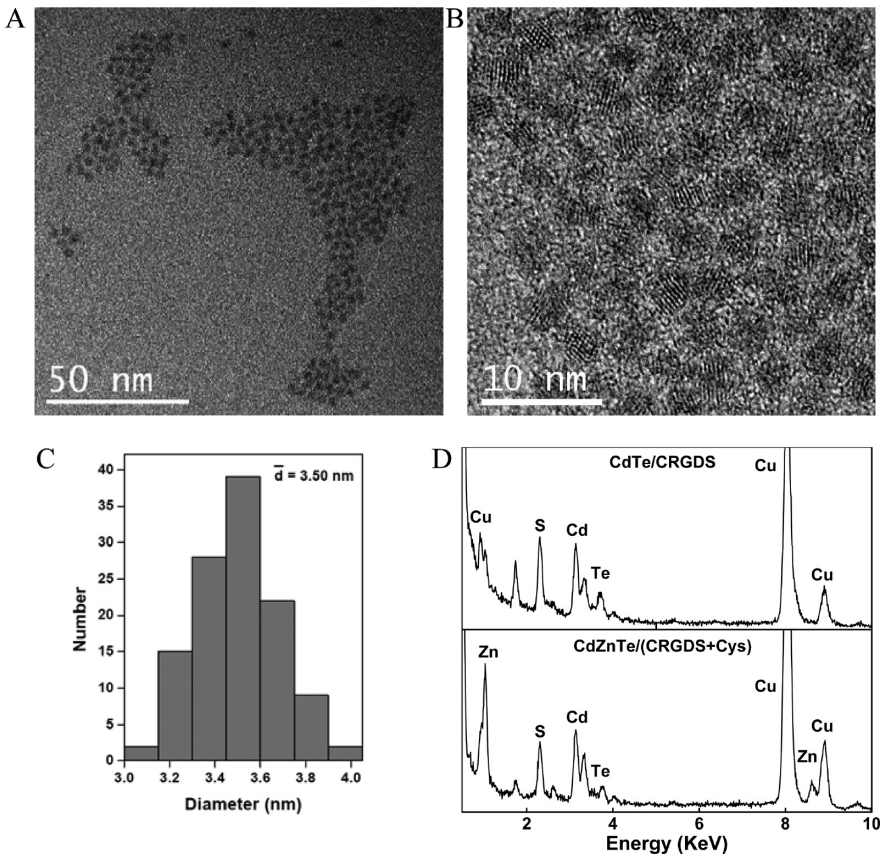

Figure 3. TEM (A) and HRTEM (B) images of (CRGDS + Cys)-capped CdZnTe QDs emitted at 590 nm. (C) Size-distribution histogram of QD determined by measuring more than 100 particles in HRTEM images. (D) EDS spectra of both CdTe QDs and CdZnTe QDs. The copper peaks were from the TEM copper grid. Note that in this case the ratio of CRGDS and Cys was 1:1.

synthesized QDs disappeared, and the emission intensity decreased significantly with a broad and asymmetric PL spectrum (Figure S7B in the Supporting Information). The reason is that an excessive number of stabilizers might distort the QD surface and result in deterioration of the nanocrystal quality.[42]

3.5. Synthesis and Characterization of CdZnTe QDs. The excellent optical properties of QDs always favor their practical applications. In order to further improve the optical properties of the RGD-capped QDs, zinc was introduced by the simultaneous reaction of Cd^{2+} and Zn^{2+} with NaHTe, and in this case, a mixture of CRGDS and Cys rather than only CRGDS was used as the stabilizer. Parts A and B of Figure 2 present the temporal evolution of the absorption and PL spectra of as-prepared CdZnTe QDs, respectively. The corresponding photograph of CdZnTe QD solutions irradiated

dx.doi.org/10.1021/am3020108 | ACS Appl. Mater. Interfaces 2012, 4, 6362−6370

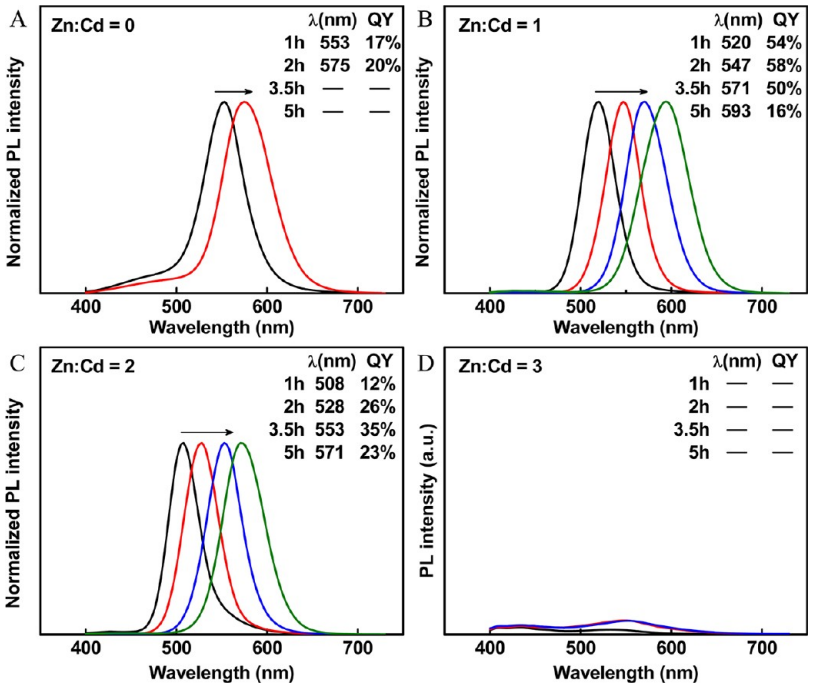

Figure 4. Temporal evolution of the PL spectra of CdTe or CdZnTe QDs at different molar ratios of zinc-to-cadmium precursors using a mixture of CRGDS and Cys as the stabilizer (1:1). The ratio of zinc to cadmium, heating time, maximum emission wavelength, and corresponding QY are also indicated.

under a UV lamp is shown in Figure 2C. The strong PL emission covering the visible range is clearly visible. Compared with the above CdTe QDs (Figure 1), these CdZnTe QDs possess obviously narrower and sharper absorption peaks and more symmetrical PL emission peaks, indicating that the optical performances of the alloyed QDs are significantly improved. Specifically, when the heating time is controlled, the PL emission wavelength of CdZnTe QDs could be tuned from 500 to 620 nm, and QYs of CdZnTe QDs above 50% were reached (Figure 2D). Note that, in addition to the alloy effect of zinc in CdTe nanocrystals, the dramatic increase in QYs was ascribed to the use of a mixture of CRGDS and Cys as the stabilizer, and such brightness could not be achieved using CRGDS or Cys alone, as shown in Figure 2D. TEM images confirmed that the RGD-functionalized CdZnTe QDs were spherical particles with excellent monodispersity, as shown in Figure 3A,B. The existence of well-resolved lattice planes in the HRTEM image confirms the crystalline structure of QDs. The size distribution determined by measuring more than 100 particles revealed that the diameter of the particles emitting at 590 nm is 3.50 ± 0.50 nm (Figure 3C). The sizes of CdZnTe QDs emitting at 534 and 570 nm are 2.96 ± 0.50 and 3.37 ± 0.40 nm, respectively (Figure S8 in the Supporting Information). Further, EDS analysis shown in Figure 3D clearly shows the presence of cadmium, zinc, tellurium, and sulfur in the sample (the sulfur was mainly from the sulfhydryl in the stabilizer).

3.6. Influence of the Ratios of Zn^{2+} to Cd^{2+} and RGD to Cys. Figure 4 presents the temporal evolution of the PL spectra of CdZnTe (or CdTe) QDs at different molar ratios of zinc-to-cadmium precursors using a mixture of CRGDS and Cys as the stabilizer. The QYs of CdZnTe QDs were significantly affected by the ratio of zinc-to-cadmium precursors. Here, a molar ratio of 1:1 for the zinc-to-cadmium precursors gave better QDs. In the absence of Zn^{2+}, the QYs of CdTe QDs were slightly improved (from 15% to 20% for the best) by only using a mixture of CRGDS and Cys as the stabilizer, as shown in Figures 4A and 1. After the incorporation of zinc into CdTe nanocrysals, the shorter bond length and stronger bond of Zn−Te can stabilize the weaker Cd−Te bond and improve the lattice structure of the nanocrystals, thus inhibiting plastic deformation and the creation of surface defects.[43,44] As a result, the as-prepared CdZnTe QDs show significantly higher QYs than CdTe QDs. A higher ratio of zinc-to-cadmium precursors, however, would decrease the QYs of the resultant QD because an excess addition of ZnTe into the CdTe lattice increases zinc-related intrinsic defects in nanocrystals.[44] In addition, because of the intermixing of the wider-band-gap Zn−Te with the narrower-band-gap Cd−Te, we can also prepare QDs that emit at different wavelengths by controlling the ratio of zinc-to-cadmium precursors. For example, when the molar ratios of zinc-to-cadmium precursors were 0, 1, and 2 (after heating for 2 h), the emission wavelengths of the as-prepared CdZnTe QDs were 575, 547, and 528 nm, respectively (Figure 4).

Figure 5 presents the absorption and PL spectra of CRGDS-capped CdZnTe QDs prepared at different molar ratios of RGD/Cys. When only CRGDS is used as the stabilizer, the best QYs of CRGDS-capped CdTe QDs or CdZnTe QDs were below 30%, suggesting that the surface of the QDs still had some defects. Compared with CRGDS, Cys is more flexible because of its short length and can further cap the surface defects. Thus, the combination of CRGDS and Cys improved the QYs of QDs. As shown in Figure 5, better QYs could be achieved over the ratios of CRGDS and Cys from 2:1 to 1:2. The highest QY of CdZnTe QDs reached was as high as 60%. Our (CRGDS + Cys)-incorporated CdZnTe-alloyed QDs exhibited excellent colloidal stability in a saturated NaCl solution and aqueous solutions with different pH values. They were also stable in water over 3 months without appreciable aggregation or a decrease in the fluorescence intensity (Figure S9 in the Supporting Information). These properties are of

dx.doi.org/10.1021/am3020108 | ACS Appl. Mater. Interfaces 2012, 4, 6362−6370

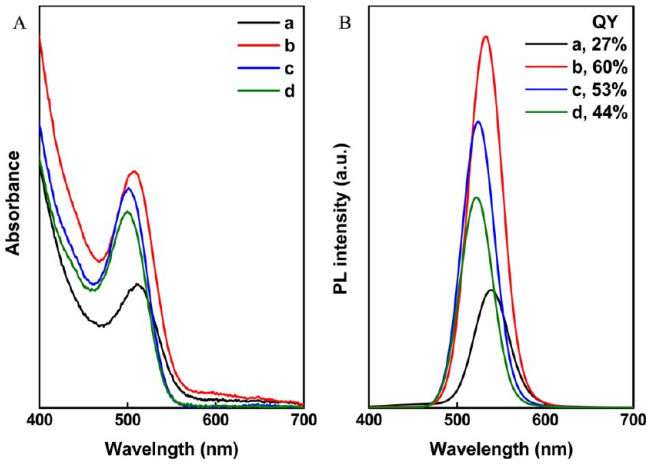

Figure 5. Absorption (A) and PL spectra (B) of CdZnTe QDs prepared using a mixture of RGD peptide and Cys with different ratios as the stabilizer after heating for 2 h.: (a) RGD:Cys = 1:0; (b) RGD:Cys = 2:1; (c) RGD:Cys = 1:1; (d) RGD:Cys = 1:2. The corresponding PL QYs are also indicated. Note that the total concentration of stabilizers was fixed at 1 mM, irrespective of the ratio variation.

significance for biological studies and applications as explained below.

3.7. Cell Imaging. The biospecificity of the as-synthesized RGD-capped QDs and their potential as luminescent probes for biological imaging were demonstrated using human cervical cancer HeLa cells (typically with overexpressing integrins[30,45]). The adherent HeLa cells were incubated with the CRGDS-capped CdTe or (CRGDS + Cys)-capped CdZnTe QDs for ~30 min at room temperature. As shown in Figure 6, the cell surface was selectively stained in both cases, as a result of the specific recognition between RGDS and cell surface integrins. On the other hand, if the cells were incubated with free RGDS first and then treated with RGD-capped QDs, no surface staining was observed because of blockage of the cell surface integrin sites by free RGDS.

Another demonstration was also conducted by incubating the suspended human leukemia cells, HL60, which also overexpressed integrins.[46] The fluorescence images of cells were taken with a digital color camera under fluorescence microscopy. In near-UV excitation, as shown in Figure 7, the luminescence (red color) of QDs was clearly distinguished from the native autofluorescence (blue color) of the cells. From these images, it was observed that the cell surface was homogeneously and specifically stained with QDs. Note that no significant cell death was observe when the two kinds of cells were incubated with QDs under the above experimental conditions. In addition, to directly assess the toxicity of QDs, we monitored the viability of HEK293, which were incubated by our RGD-peptide-capped QDs at 37 °C for 4 h. No significant cell death was observed (Figure S10 in the Supporting Information), suggesting little cytotoxicity associated with our RGD-capped QDs under the given experimental conditions.

4. CONCLUSIONS

We have demonstrated the convenient one-pot aqueous synthesis of integrin-binding QDs by using designed short RGD peptides as stabilizers. The effects of different RGD peptides on the synthesis of CdTe QDs were examined. By optimizing short peptide primary structures and reaction conditions, the best QY of CdTe QDs was 15%, with narrow fwhm values of 40−60 nm. In order to further improve the optical properties of QDs, we prepared successfully RGD-functionalized alloyed CdZnTe QDs by the simultaneous reaction of Cd^{2+} and Zn^{2+} with NaHTe using a mixture of

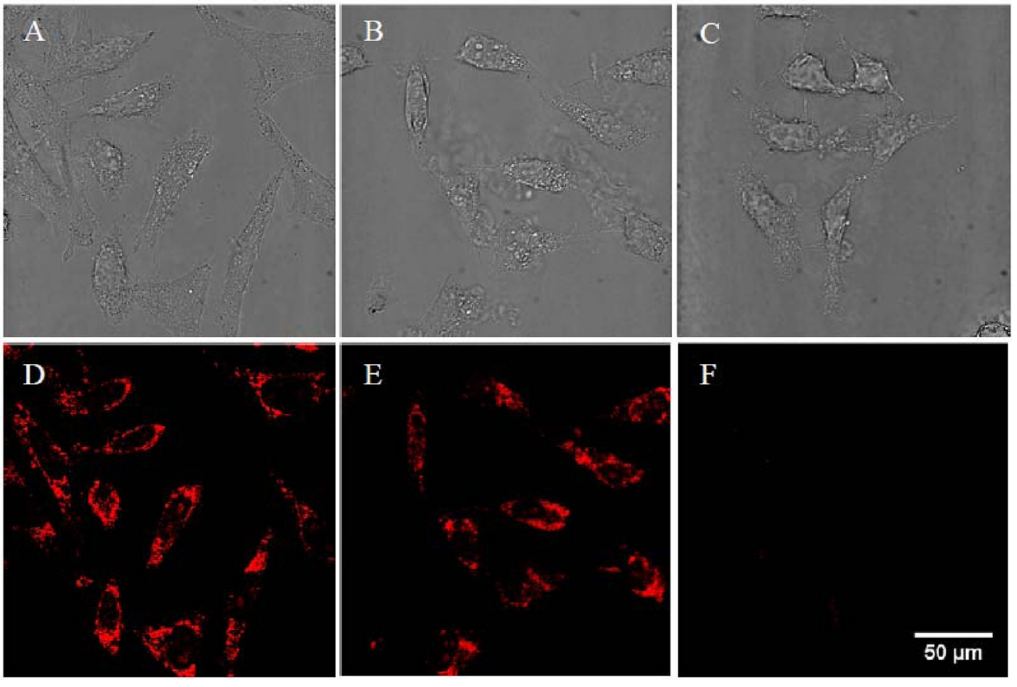

Figure 6. Bright-field (upper panel) and confocal fluorescence images (lower panel) of HeLa cells incubated with (A and D) CRGDS-capped CdTe QDs emitted at 575 nm, (B and E) (CRGDS + Cys)-capped CdZnTe QDs emitted at 575 nm, and (C and F) the same CRGDS-capped CdTe QDs following prior incubation with free RGDS. All fluorescence images were displayed under the same scale.

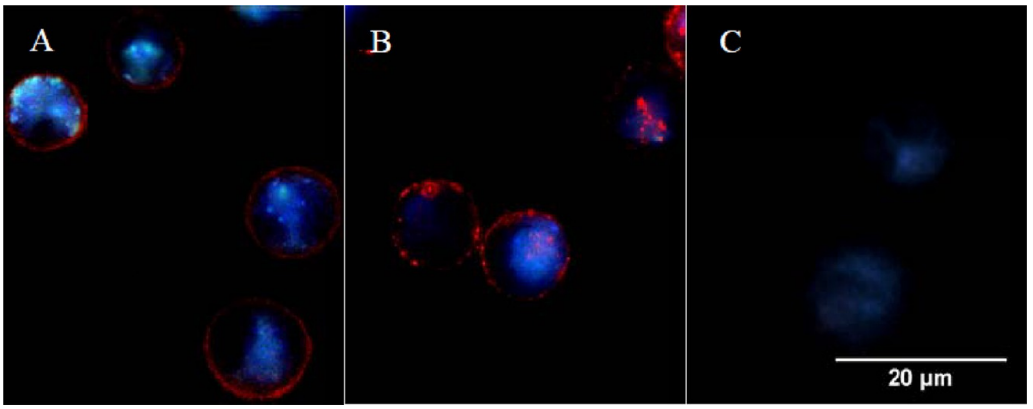

Figure 7. Fluorescence images of HL60 cells incubated with (A) CRGDS-capped CdTe QDs emitted at 575 nm, (B) (CRGDS + Cys)-capped CdZnTe QDs emitted at 575 nm, and (C) the same CRGDS-capped CdTe QDs after the prior incubation with free RGDS. Note that the images were taken with a digital color camera under fluorescence microscopy. The blue color is the native autofluorescence of the cells in near-UV excitation, and the red color is the luminescence of QDs.

CRGDS and Cys as the stabilizer. Under optimum conditions, the PL QY of CdZnTe alloy QDs reached as high as 60%. Furthermore, these QDs were found to be biocompatible and stable under physiological conditions. More importantly, they also showed a high efficacy for attachment to the cell surface due to the specific recognition between RGDS and the cell surface integrin receptors. Besides the advantage of avoiding complicated synthetic steps, the newly developed strategy has opened up a new and facile avenue to directly synthesizing biospecific QDs in aqueous solution using designed short peptides, enabling easy surface attachment of more specific and elaborate sequences or motifs to QD surfaces for targeting certain cells or cellular organelles.

■ ASSOCIATED CONTENT

Supporting Information

Figures S1−S10. This material is available free of charge via the Internet at http://pubs.acs.org.

■ AUTHOR INFORMATION

Corresponding Author

*Phone: 86-532-86981569 (H.X.), 44-161-2003926 (J.R.L.). E-mail: xuh@upc.edu.cn (H.X.), j.lu@manchester.ac.uk (J.R.L.).

Notes

The authors declare no competing financial interest.

■ ACKNOWLEDGMENTS

This work was supported by the National Natural Science Foundation of China under Grant 20905078, the Natural Science Foundation of Shandong Province under Grant ZR2009BQ001, and the Fundamental Research Funds for the Central Universities under Grant 27R1204029A. H.X. acknowledges support by the Program for New Century Excellent Talents in University (Grant NCET-11-0735). We also thank UK Engineering and Physical Sciences Research Council (EPSRC) for support under Grants KTP008143 and EP/F062966/1.

■ REFERENCES

(1) Bruchez, M.; Moronne, M.; Gin, P.; Weiss, S.; Alivisatos, A. P. *Science* **1998**, *281*, 2013−2016.
(2) Michalet, X.; Pinaud, F. F.; Bentolila, L. A.; Tsay, J. M.; Doose, S.; Li, J. J.; Sundaresan, G.; Wu, A. M.; Gambhir, S. S.; Weiss, S. *Science* **2005**, *307*, 538−544.
(3) Medintz, I. L.; Uyeda, H. T.; Goldman, E. R.; Mattoussi, H. *Nat. Mater.* **2005**, *4*, 435−446.
(4) Murray, C. B.; Norris, D. J.; Bawendi, M. G. *J. Am. Chem. Soc.* **1993**, *115*, 8706−8715.
(5) Peng, Z. A.; Peng, X. *J. Am. Chem. Soc.* **2001**, *123*, 183−184.
(6) Larson, D. R.; Zipfel, W. R.; Williams, R. M.; Clark, S. W.; Bruchez, M. P.; Wise, F. W.; Webb, W. W. *Science* **2003**, *300*, 1434−1436.
(7) Wu, X.; Liu, H.; Liu, J.; Haley, K. N.; Treadway, J. A.; Larson, J. P.; Ge, N.; Peale, F.; Bruchez, M. P. *Nat. Biotechnol.* **2003**, *21*, 41−46.
(8) Gao, X.; Cui, Y.; Levenson, R. M.; Chung, L. W.; Nie, S. *Nat. Biotechnol.* **2004**, *22*, 969−976.
(9) Chan, W. C.; Nie, S. *Science* **1998**, *281*, 2016−2018.
(10) Jaiswal, J. K.; Mattoussi, H.; Mauro, J. M.; Simon, S. M. *Nat. Biotechnol.* **2003**, *21*, 47−51.
(11) Mattoussi, H.; Mauro, J. M.; Goldman, E. R.; Anderson, G. P.; Sundar, V. C.; Mikulec, F. V.; Bawendi, M. G. *J. Am. Chem. Soc.* **2000**, *122*, 12142−12150.
(12) Talapin, D. V.; Rogach, A. L.; Mekis, I.; Haubold, S.; Kornowski, A.; Haase, M.; Weller, H. *Colloids Surf., A* **2002**, *202*, 145−154.
(13) Pons, T.; Uyeda, H. T.; Medintz, I. L.; Mattoussi, H. *J. Phys. Chem. B* **2006**, *110*, 20308−20316.
(14) Gaponik, N.; Talapin, D. V.; Rogach, A. L.; Hoppe, K.; Shevchenko, E. V.; Kornowski, A.; Eychmuller, A.; Weller, H. *J. Phys. Chem. B* **2002**, *106*, 7177−7185.
(15) Li, L.; Qian, H.; Fang, N.; Ren, J. *J. Lumin.* **2005**, *116*, 59−66.
(16) Li, L.; Qian, H.; Ren, J. *Chem. Commun.* **2005**, 528−530.
(17) Rogach, A. L.; Franzl, T.; Klar, T. A.; Feldmann, J.; Gaponik, N.; Lesnyak, V.; Shavel, A.; Eychmueller, A.; Rakovich, Y. P.; Donegan, J. F. *J. Phys. Chem. C* **2007**, *111*, 14628−14637.
(18) Wang, S.; Mamedova, N.; Kotov, N. A.; Chen, W.; Studer, J. *Nano Lett.* **2002**, *2*, 817−822.
(19) Li, Y.; Duan, X.; Jing, L.; Yang, C.; Qiao, R.; Gao, M. *Biomaterials* **2011**, *32*, 1923−1931.
(20) Yong, K. T.; Roy, I.; Law, W. C.; Hu, R. *Chem. Commun.* **2010**, *46*, 7136−7138.
(21) Li, Y.; Jing, L.; Qiao, R.; Gao, M. *Chem. Commun.* **2011**, *47*, 9293−9311.
(22) Ma, N.; Tikhomirov, G.; Kelley, S. O. *Acc. Chem. Res.* **2010**, *43*, 173−180.
(23) Ma, N.; Yang, J.; Stewart, K. M.; Kelley, S. O. *Langmuir* **2007**, *23*, 12783−12787.
(24) Ma, N.; Sargent, E. H.; Kelley, S. O. *Nat. Biotechnol.* **2009**, *4*, 121−125.

(25) Tikhomirov, G.; Hoogland, S.; Lee, P. E.; Fischer, A.; Sargent, E. H.; Kelley, S. O. *Nat. Nanotechnol.* **2011**, *6*, 485−490.
(26) Zhao, X.; Pan, F.; Xu, H.; Yaseen, M.; Shan, H.; Hauser, C. A.; Zhang, S.; Lu, J. R. *Chem. Soc. Rev.* **2010**, *39*, 3480−3498.
(27) Pierschbacher, M. D.; Ruoslahti, E. *Nature* **1984**, *309*, 30−33.
(28) Ruoslahti, E.; Pierschbacher, M. D. *Science* **1987**, *238*, 491−497.
(29) Lieleg, O.; Lopez-Garcia, M.; Semmrich, C.; Auernheimer, J.; Kessler, H.; Bausch, A. R. *Small* **2007**, *3*, 1560−1565.
(30) Ko, M. H.; Kim, S.; Kang, W. J.; Lee, J. H.; Kang, H.; Moon, S. H.; Hwang, D. W.; Ko, H. Y.; Lee, D. S. *Small* **2009**, *5*, 1207−1212.
(31) Cai, W.; Chen, X. *Nat. Protoc.* **2008**, *3*, 89−96.
(32) Smith, B. R.; Cheng, Z.; De, A.; Koh, A. L.; Sinclair, R.; Gambhir, S. S. *Nano Lett.* **2008**, *8*, 2599−2606.
(33) Xu, H.; Wang, J.; Han, S.; Yu, D.; Zhang, H.; Xia, D.; Zhao, X.; Waigh, T. A.; Lu, J. R. *Langmuir* **2009**, *25*, 4115−4123.
(34) Wang, J.; Han, S.; Meng, G.; Xu, H.; Xia, D.; Zhao, X.; Schweins, R.; Lu, J. R. *Soft Matter* **2009**, *5*, 3870−3878.
(35) Chen, C.; Pan, F.; Zhang, S.; Hu, J.; Cao, M.; Wang, J.; Xu, H.; Zhao, X.; Lu, J. R. *Biomacromolecules* **2010**, *11*, 402−411.
(36) Yu, W. W.; Qu, L.; Guo, W.; Peng, X. *Chem. Mater.* **2003**, *15*, 2854−2860.
(37) Winter, J. O.; Liu, T. Y.; Korgel, B. A.; Schmidt, C. E. *Adv. Mater.* **2001**, *13*, 1673−1677.
(38) Spoerke, E. D.; Voigt, J. A. *Adv. Funct. Mater.* **2007**, *17*, 2031−2037.
(39) Zhang, H.; Zhou, Z.; Yang, B.; Gao, M. *J. Phys. Chem. B* **2002**, *107*, 8−13.
(40) Park, Y. S.; Dmytruk, A.; Dmitruk, I.; Kasuya, A.; Takeda, M.; Ohuchi, N.; Okamoto, Y.; Kaji, N.; Tokeshi, M.; Baba, Y. *ACS Nano* **2010**, *4*, 121−128.
(41) Qian, H.; Dong, C.; Weng, J.; Ren, J. *Small* **2006**, *2*, 747−751.
(42) Borchert, H.; Talapin, D. V.; Gaponik, N.; McGinley, C.; Adam, S.; Lobo, A.; Möller, T.; Weller, H. *J. Phys. Chem. B* **2003**, *107*, 9662−9668.
(43) Bell, S. L.; Sen, S. *J. Vac. Sci. Technol., A* **1985**, *3*, 112−115.
(44) Li, W.; Liu, J.; Sun, K.; Dou, H.; Tao, K. *J. Mater. Chem.* **2010**, *20*, 2133−2138.
(45) Sheu, J. R.; Lin, C. H.; Peng, H. C.; Huang, T. F. *Peptides* **1994**, *15*, 1391−1398.
(46) Anuradha, C. D.; Kanno, S.; Hirano, S. *Cell Biol. Toxicol.* **2000**, *16*, 275−283.